

João F. Mano
Jean-Marc Saiter

Using mechanical spectroscopies to study the glass transition dynamics in unsaturated polyester resins cured with different styrene contents

Received: 16 April 2004
Accepted: 2 September 2004
Published online: 28 October 2004
© Springer-Verlag 2004

J. F. Mano (✉)
Department of Polymer Engineering,
University of Minho, Campus de Azurém,
4800-058 Guimarães, Portugal
E-mail: jmano@dep.uminho.pt
Tel.: +351-2-53510320
Fax: +351-2-53510339

J. F. Mano
3B's Research Group—Biomaterials,
Biodegradables and Biomimetics,
University of Minho, Campus de Gualtar,
4710-057 Braga, Portugal

J.-M. Saiter
LECAP, PBM UMR6522, Faculté des
Sciences, Université de Rouen, site du
Madrillet, Avenue de l'Université, BP12,
76801 Saint Etienne du Rouvray, France

Abstract The control of chemical architecture has been one relevant parameter in the study of glass transition dynamics in macromolecular systems. In this study, two polyester resins differing in the styrene content that was added in the curing process were studied using two complementary mechanical spectroscopy techniques: dynamic mechanical analysis (DMA) and thermally stimulated recovery (TSR). Both techniques showed that the α -relaxation is shifted to higher temperatures (longer times) with increasing styrene content. Master curves were obtained from the DMA data. The shift factors were used to obtain the temperature dependence of the apparent activation energy, $E_a(T)$. The TSR results also permit-

ted to obtain $E_a(T)$ that also exhibited a maximum around T_g . This behaviour, apparently universally observed in thermally stimulated techniques, was explained by the shift from a Vogel-Fulcher-Tammann-Hesse to an Arrhenius regime. The data also allowed to calculate the fragility index of the two materials, which was found to be higher for the one with higher styrene content. Remarks are made on the dependency of the values of this parameter obtained from different techniques.

Keywords DMA · TSR · Segmental mobility · Relaxations · Thermoset polymers

Introduction

The molecular mechanisms assigned to the occurrence of glass transition are extremely complex and remain one of the most important unsolved problems concerning condensed matter physics. A huge number of papers and dedicated meetings have discussed this issue from both an experimental and theoretical point of view [1–5]. Experimentally, the vitrification process may be monitored through the change of different physical/thermodynamic properties, such as heat capacity, thermal expansivity, dielectric permittivity or modulus. Here, it has long been recognised that the frequency or time dependence on the observed dynamics should also be

mapped out to gain deeper insights on the kinetic nature of glass transition [6]. One may change the time scale of experiments either by changing the frequency (isothermal) of the external excitation or temperature (for a fixed frequency), and measure the corresponding response. Examples of such dynamic techniques are dielectric spectroscopy or mechanical spectroscopy (or dynamic mechanical analysis—DMA), where a wide range of frequencies are accessible. Alternatively, quasi-static techniques may be used, which usually give access to low-frequency information. In the mechanical area, creep and stress relaxation are tools frequently used to probe molecular mobility in the time domain [7]. In this context, it has been shown that isothermal conventional

quasi-static mechanical tests can be used to study glass transition dynamics, and the corresponding equivalent frequency may be estimated [8]. Transient-like tests may also be performed under non-isothermal conditions, where a static stimulus is imposed on the sample and the response is measured while the sample is heated, usually at a constant rate. The thermally stimulated depolarisation current technique (TSDC) is the most used, where the polarisation release of a previously poled sample at higher temperatures is measured as a function of temperature, during heating at a constant rate [9]. The mechanical equivalents of this technique are the thermally stimulated creep (TSCreep) or thermally stimulated recovery (TSR), which were found to give complementary information with respect to the dynamic data [10, 11].

A good strategy that contributes to the understanding of the glass transition phenomenon is to analyse systems with different and controllable chemical structures and microstructures. Unsaturated polyester resins (UPR) cured with different styrene contents are widely used in the coating technology area and constitute an adequate system for such a study of glass transition dynamics as a function of chemical architectures [12]. In fact, such thermosets may be easily adapted to specific applications by changing either the nature of the unsaturated polyester chain or the ratio of the amounts of styrene/polyester, therefore making them adequate for systematic studies of glass transition dynamics. In this work, the viscoelastic properties in the glass transition region, of two materials differing in the styrene content, will be compared, using both dynamic and transient-like techniques. Both DMA and TSR results, obtained in the same equipment and operative conditions will be compared.

Experimental

TECHNIBAT CO. (Gravigny, France) provided the UPR studied in this work. The polyester resins consist of maleic anhydride (1 mol), isophthalic acid (1 mol) and propylene glycol (2 mol) mixed in styrene monomer solution. The initiator was methylethylketone peroxide (MEKP, AKZO) and the promoter was cobalt octoate (AKZO). To initiate the reaction, 0.2% (w/w) of the promoter solution which contains 6% (w/w) of cobalt octoate was first mixed with the resin. Then 1.5% (w/w) of the initiator solution was added to the mixture (resin + styrene + promoter). According to the method described elsewhere [13], the thermal cycle performed to obtain the solid state consisted of isothermal curing at 25 °C for 24 h followed by a post curing at 80 °C for 6 h and a second post curing of 2 h at 120 °C. With this method the maximum degree of transformation is reached. In order to perform the mechanical experi-

ments, bulk materials (rods) were obtained by adequate moulding conditions. Two materials were studied in this work, differing only in the styrene content: 0.25 and 0.38 (w/w), labelled in this work as UPR25 and UPR38, respectively.

Both the DMA and TSR experiments were carried out in a DMA7e Perkin-Elmer analyser with controlled cooling accessory. A continuous flux of high purity helium (flow rate of $\sim 65 \text{ cm}^3 \text{ min}^{-1}$) was used to improve heat transfer throughout the sample surroundings during the experiments.

The experiments on the polymer were carried out with the three point bending mode. The sample was placed over a 15-mm bending platform, and a 5-mm knife-edge probe tip provided the mechanical excitation.

The DMA experiments were performed in isothermal conditions, at different temperatures, from 48.8 to 115.4 °C every 3 °C. At each temperature the frequency was scanned from 0.8 to 20 Hz. The dynamic stresses applied were such that the provided measurements were within the viscoelastic linear regime.

Using the TSR technique one may perform at least two kinds of experiments: the TSR global and the thermal sampling (TS) (or windowing) experiments. In both types of experiments a static stress, σ_0 , is applied in a given temperature range after an isothermal period (between T_σ and $T_\sigma - \Delta T_w$). Then the strain is frozen-in by cooling down to T_0 , without any stress, and the strain is measured, as a function of the temperature, on heating at a constant rate ($q^+ = dT/dt$) up to a temperature well above T_σ . The difference between both experiments is that in a TSR global experiment $\Delta T_w = T_0$, whereas in a TS experiment $\Delta T_w \sim 3^\circ\text{C}$ and $T_0 < T_\sigma$. In all the experiments carried out in this work, we used $q^+ = 4^\circ\text{C min}^{-1}$ and for the TS experiments $\Delta T_w = 3^\circ\text{C}$. All coolings were performed at $20^\circ\text{C min}^{-1}$. More details on the experimental procedures may be found in one of our previous works [10].

In the TSR global experiments, the complex nature of the relaxation is studied because conformational motions are activated with a certain characteristic time between T_σ and T_0 . On the other hand, the TS experiments allow to resolve the complex relaxational spectrum. Each TS curve can be analysed as a thermostimulated mechanical recovery process of an elementary mechanism, because only the processes within a narrow temperature range are activated. The ensemble of the TS experiments within the glass transition region gives an overall picture of the processes associated with the relaxation as probed at low frequencies.

In this work, the temperature correction was performed using the procedures described in Reference [14]. For the DMA experiments, the measured temperatures of ice melting were extrapolated to zero heating rate, while for the TSR experiments, the data for $q^+ = 4 \text{ K min}^{-1}$ were used directly.

Results

Dynamic mechanical analysis

Isothermal DMA data was collected for both UPR25 (from 60.8 to 110.1 °C) and UPR38 (from 48.8 to 115.4 °C), in the region of their glass transition. The storage and loss moduli (E' and E'') for the two materials are shown in Figs. 1 and 2, for most temperatures analysed. These results were used to plot isochronal data for the two materials. In Fig. 3, for example, both E' and E'' are represented as a function of temperature for a frequency of 1 Hz. The E'' curves permit to conclude that the glass transition of UPR38 is higher than UPR25 (temperature of maximum E'' is 76 and 85 °C for UPR25 and UPR38, respectively). The increase of the value of the glass transition temperature by increasing the styrene content is the expected behaviour. Indeed, as

demonstrated by Bureau et al. [12] and by Delahaye et al. [13], the increase of the styrene content allows to increase the styrenic chain length bonded to the maleic chain and progressively the properties of the mixture tends toward the characteristic of a polystyrene material. From the DSC results, it was found that the difference on the T_g 's was about 12 °C (83 and 95 °C for UPR25 and UPR38, respectively, obtained at 10 °C min⁻¹) [12]. At this stage of the data presentation, we have to also say that with this value of q^+ , the glass transition observed on a DSC trace occurs on a very broad temperature domain ($\Delta T_g = 71 \pm 11$ °C and $\Delta T_g = 69 \pm 4$ °C for UPR25 and UPR38, respectively) [12]. Another feature found in Fig. 3 is the higher values of E' for UPR25 in the glassy state (lower temperatures) than for UPR38.

The time-temperature correspondence principle may be used in the results of Figs. 1 and 2 to obtain the viscoelastic information in a wide frequency range, by

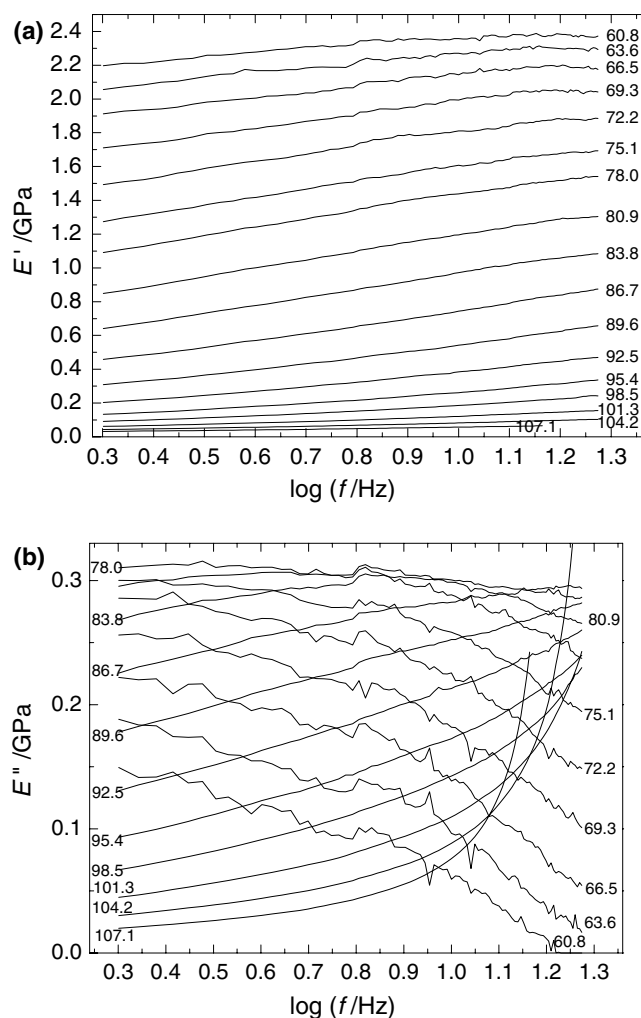


Fig. 1 Dynamic mechanical analysis isothermal curves for UPR25 at different temperatures (in the graphics in °C). **a** storage modulus versus frequency, **b** loss modulus versus frequency

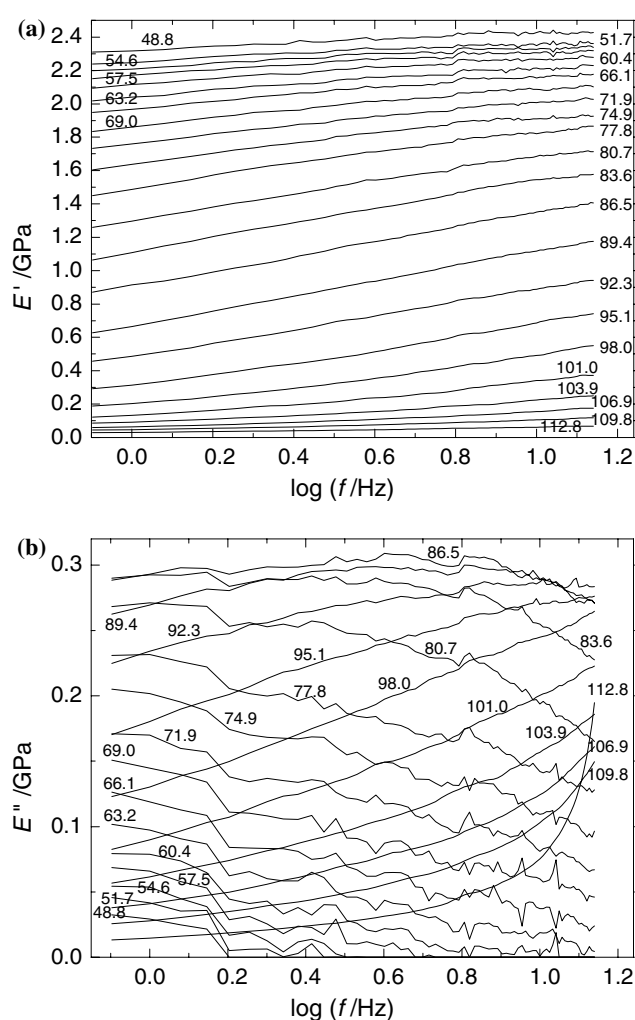


Fig. 2 Dynamic mechanical analysis isothermal curves for UPR38 at different temperatures (in the graphics in °C). **a** storage modulus versus frequency, **b** loss modulus versus frequency

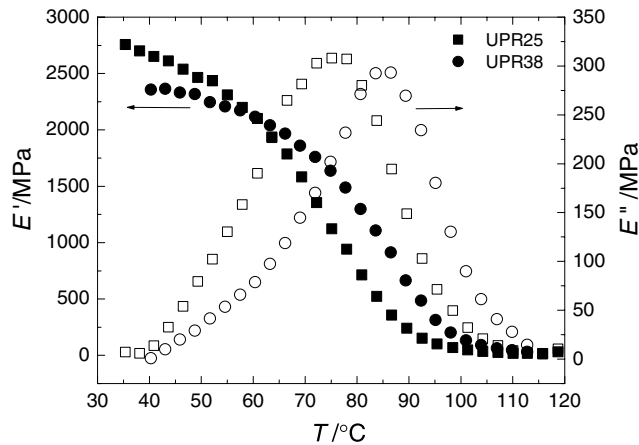


Fig. 3 Storage and loss moduli (filled and open symbols, respectively) of UPR25 (squares) and UPR38 (circles) at 1 Hz, extracted from the isothermal data (Figs. 1 and 2), as a function of temperature

simple horizontal shifting of the data [7]. Master curves of E' for UPR25 and UPR38 are shown in Fig. 4, for reference temperatures T_{ref} of 92.5 and 92.3 °C, respectively. In principle, a small vertical shift due to the temperature dependence of $\rho T/\rho_{\text{ref}}T_{\text{ref}}$ should also be applied [7], but in this case the correction seemed to be negligible. As expected, the results in Figs. 3 and 4 are consistent. For example, it is clear from the master curves that UPR25 has been shifted to higher frequencies (lower times) than UPR38, indicating faster segmental motions.

The temperature shift factors, $\log a_T$, associated with the construction of the master curves contain information

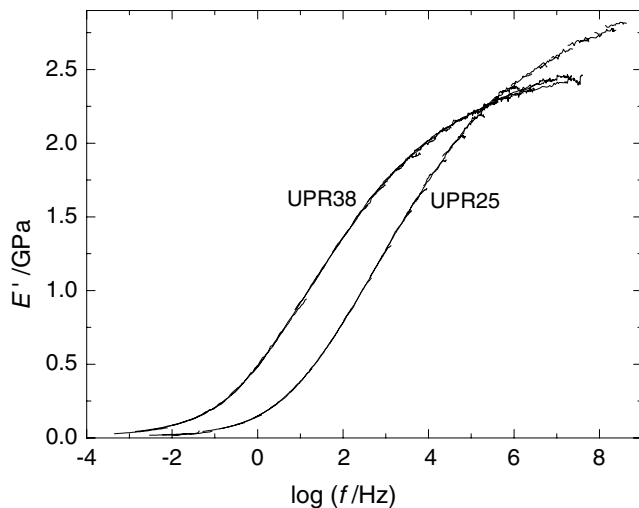


Fig. 4 Master curve for the storage modulus of UPR25 and UPR38 obtained from horizontal displacements of the data in Figs. 1 and 2, for reference temperatures 92.5 and 92.3 °C, respectively

about the glass transition dynamics. In the present study, one is interested in comparing dynamic results with TSR. The characteristic times assigned to the TSR response correspond to retardation times, as we are measuring the temperature dependence of a susceptibility quantity (strain for a given fixed stress applied during the creep period). The characteristic times associated with the temperature shift factor of E' are relaxation times. These may be changed to the corresponding retardation times (that are related to the mechanical compliance data, $D^* = D' - i D''$) taking into account that the dynamic information contained in E' and D' (or E'' and D'') are equivalent but shifted in the temperature axis. Therefore, the $\log a_T$ versus T for the retardation times were obtained from the data taken from the E' master curve but shifted to higher temperatures, corresponding to the difference in the temperature axis of the maximum of D'' and E'' , for the same frequency. The isochronal data for D'' at 1 Hz is shown in the inset of Fig. 5. It was found that the maximum of D'' is located 36.9 °C above the E'' peak, for both UPR25 and UPR38. Figure 5 represents the temperature dependence of $\log a_T$ for the retardation times.

The results will be used to calculate the temperature dependence of the activation energy, which will be compared with the TSR data.

Thermally stimulated recovery

Figure 6 shows some TS curves obtained from 62.7 to 105.6 °C for UPR25 and between 61.8 and 103.7 °C for UPR38. The data represents the normalised strain (with respect to the creep stress) as a function of temperature.

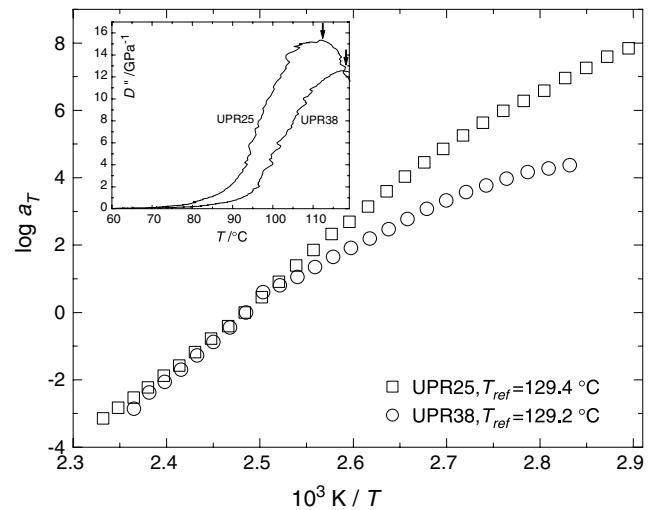


Fig. 5 Temperature shift factor assigned to the retardation times, for UPR25 (squares) and UPR38 (circles) for reference temperatures of 129.4 and 129.2 °C, respectively. Inset graphics: D'' as a function of temperature for a frequency of 1 Hz

For all the samples, the curves are shifted to higher temperatures when T_σ increases, due to the fact that the relaxational modes that are isolated correspond to modes that, for the equivalent time of the TS experiments ($\sim 10^2$ – 10^3 s [15]), are active around T_σ , i.e. will be released during heating at increasing temperatures with increasing T_σ .

The anelastic response associated to each TS curve is usually analysed as a quasi-elementary process, often modelled with a Voigt-Kelvin model. The temperature dependence of the retardation times of such curves are obtained up to near the temperature of maximum strain-rate using the relationship that is derived from the $\epsilon(T)$ expression taken from the Voigt-Kelvin model:

$$\tau(T) = \frac{1}{q^+} \left[\frac{\epsilon(T)}{|d\epsilon(T)/dT|} \right] \quad (1)$$

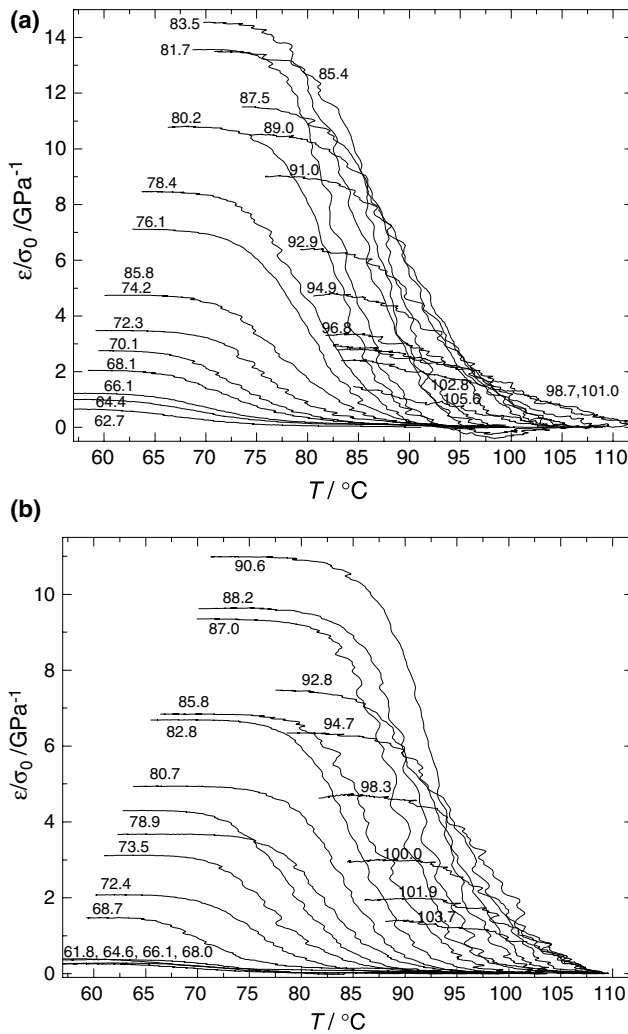


Fig. 6 Normalised strain obtained during TS experiments on UPR25 (a) and UPR38 (b) at different creep temperatures T_σ (in the graphics, in °C)

where q^+ is the heating rate. Usually, an Arrhenius dependence of $\tau(T)$ is assumed :

$$\ln \tau(T) = \ln \tau_0 + \frac{E_a}{RT} \quad (2)$$

which permits to obtain both the activation energy, E_a , and the pre-exponential factor, τ_0 , of each TS curve, from a linear regression of $\ln \tau(T)$ versus $1/T$. More details about the calculation of the thermokinetic parameters may be found in a previous work [10]. Therefore, $\tau(T)$ curves were obtained for the two materials for each T_σ analysed (not shown), that allowed to determine E_a for each TS experiment. In the next section, such results will be analysed. It should be emphasised that Eq. 1 is only valid for relaxation processes arising from an infinitely narrow distribution of characteristic times. Therefore, errors are always committed when one is dealing with experimental results, where the TS procedure is never capable of completely isolating a complex relaxation into individual components. However, these errors may be minimised, for example, by using only the initial part of the $\epsilon(T)$ curve, up to the temperature of inflexion [10].

Discussion

Figure 7 shows the apparent activation energy obtained for the two materials with TSR (symbols), as a function of T_{\max} , the temperature of maximum strain rate (i.e. the temperature at which $d\epsilon/dT$ presents a maximum); T_{\max} accompanies the trend of T_σ , though exhibiting higher values, and better describes the temperature of the process as it corresponds to the temperature at which the previously isolated modes relax faster. An increase of E_a is observed with increasing T_σ in the glassy region of the transition, followed by a decrease in the equilibrium state. In order to explain this behaviour, one should consider the general temperature evolution of the characteristic times around T_g in glass-forming systems, as well as the existence of a distribution of times. An explanation has already been given elsewhere [16], but it will be again briefly discussed here.

Figure 8 shows schematically $\log \tau$ versus $1/T$. The $\langle \tau \rangle$ line corresponds to the mean retardation time, and the distribution of times is represented by the intensity of the bands around the $\langle \tau \rangle$ curves (obviously, in reality we should have a continuous intensity gradient). Darker colour for corresponds to higher values for the probability density function, which, as expected, occurs near $\langle \tau \rangle$. We will consider here a thermorheological simple system, where the shape of the distribution of retardation times does not change with temperature.

With TS experiments one isolates the retardation times that at T_σ are around the characteristic times of the technique (around 100 s [15]). In fact, longer times

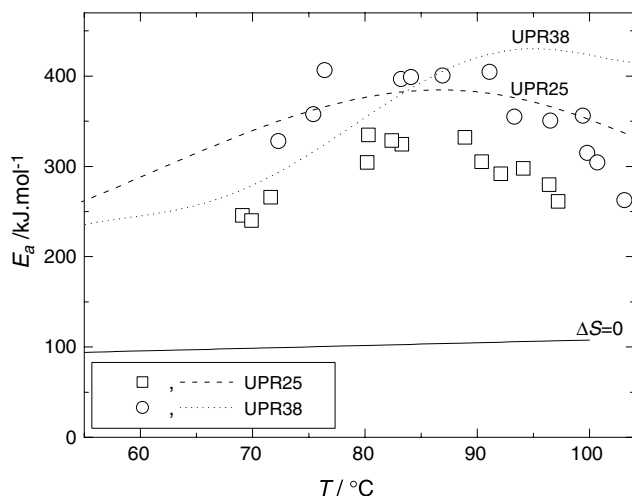


Fig. 7 Temperature dependence of the apparent activation energy obtained by TS experiments for UPR25 (squares) and UPR38 (circles), represented as a function of temperature of maximum strain rate, T_{\max} , and by DMA (dashed and dotted lines for UPR25 and UPR38, respectively), obtained from numerical derivation of the shift factor data (Fig. 5). The solid line is the prediction for a zero-entropy case (non-cooperative processes)—see text

are not activated within the creep time at T_σ and shorter ones are relaxed at $T_\sigma - \Delta T_w$, during the isothermal recovery stage. Therefore, as T_σ increases from the glassy to the liquid regions of the glass transition, TS curves are probing narrow distributed molecular motions at a time scale of ~ 100 s, scanning the broad distribution of retardation times in an horizontal way (dotted line in Fig. 8), rather than the vertical scanning of isothermal dynamic tests. Figure 8 represents this distribution of “glass transition temperatures” (dashed line) of the variety of modes that may be activated at such equivalent frequencies. The general shape of the $\langle \tau \rangle$ line will be discussed now. At higher temperatures, it follows a Vogel-Fulcher-Tamman-Hesse equation (VFTH) [17–19]:

$$\ln \tau(T) = \ln \tau_0 + \frac{B}{T - T_0}, \quad T_0 < T_g \quad (3)$$

where τ_0 is a pre-exponential factor and B and T_0 are adjustable parameters. When the temperature decreases throughout the glassy state, the VFTH behaviour gradually tends to an Arrhenius behaviour (Eq. 2). Therefore, the curvature in the relaxation plot of Fig. 8 should tend to be a straight line with decreasing temperature. The global shape of the characteristic times in the temperature axis shown in Fig. 8 helps to justify the trend in $E_a(T)$ found in Fig. 7 for the TS data. In the glassy region, one is isolating the modes that tend, at lower temperatures, to follow the Arrhenius behaviour (lower apparent activation energy). With increasing T_σ , the trend adopts progressively the VFTH behaviour,

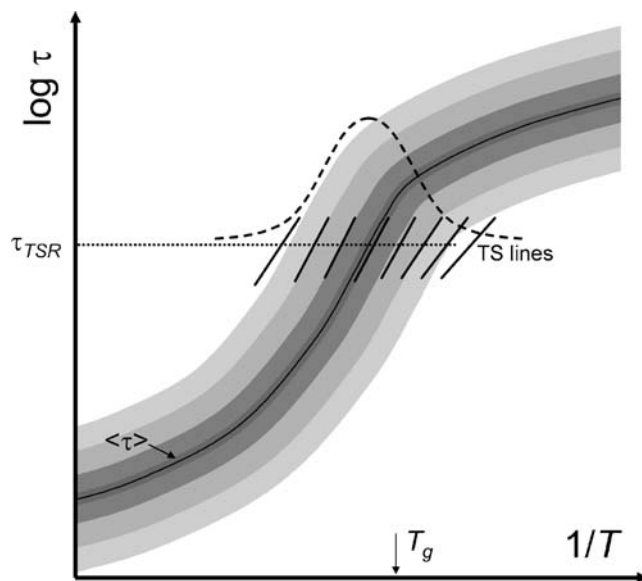


Fig. 8 Scheme representing the evolution of the characteristic times around T_g . $\langle \tau \rangle$ is the mean retardation time and the different bands around this line represent the intensity (higher for increasing darkness) of the probability density function for the retardation times. The dashed curve represents the distribution of modes that are active with retardation times equivalent to the TSR experiments ($\tau_{TSR} \sim 100\text{--}1,000$ s), as a function of temperature. The line segments represent typical Arrhenius plots obtained from TS experiments at different T_σ

and thus the activation energy increases (see straight lines representing Arrhenius TS lines in Fig. 8). However, for higher values of T_σ in the equilibrium state, the apparent activation energies should decrease with increasing T_σ as the times follow a VFTH regime. Therefore, an increase of E_a would be expected followed by a decrease around T_g , as T_σ increases. This is in fact what we observe in Fig. 7 for both UPR25 and UPR38 (symbols). As expected, the maximum of E_a occurs at higher temperatures for UPR38 as its T_g is higher. It should be pointed out that such a trend in $E_a(T)$ has also been found in TSDC experiments (e.g. [20–22]), although to our knowledge such explanations have never been provided.

An apparent activation energy plot may also be obtained from the dynamic data, by differentiating the shift factors, shown in Fig. 5:

$$E_a(T) = R(\ln 10) \frac{d \log a_T}{d T^{-1}} \quad (4)$$

Here the $E_a(T)$ trend should follow the shape of the slope of the $\langle \tau \rangle$ line shown in Fig. 8, where again a maximum is observed near T_g , on the transition between the VFTH and Arrhenius regimes. The maxima of the $E_a(T)$ data obtained by TSR and DMA do not coincide in the temperature axis. Such behaviour was observed in other systems and assigned to the different thermal

history of the samples during the two kinds of experiments [16, 23]. Figure 8 also suggests that the activation energies obtained by dynamic data are higher than the ones obtained by TSR. A possible explanation could be related to the non-exponential response of the glass transition dynamics. It was suggested that for systems that relax with time according to a stretch-exponential form (i.e. $\exp[-(t/\tau)^\beta]$), the parameter determined by most of the methods is not the activation energy, but rather the product βE_a [24]. This could mean that we could be measuring an activation energy lower than the true one.

Figure 8 may also be useful to understand the variation of the low temperature values of ϵ/σ_0 (in the plateau) with T_σ (see Fig. 6). The results suggest that such values increase with T_σ in the glassy state and, above 84.5 and 90.6 °C for UPR25 and UPR38, respectively, they start to decrease. As mentioned previously, during TS experiments one isolates modes with characteristic times around 100 s that are active at T_σ . For low values of T_σ , one is in the glassy region and the number of modes exhibited by such time scales is scarce; the same applies for temperatures much above T_g , where most of the segmental motions are much faster (lower τ). The dashed line in Fig. 8 represents the distribution of modes that are active at the TSR equivalent times. It is clearly seen that the values of T_σ that could activate more modes are obtained when the experiments are performed around T_g . That is the reason why the permanent deformation that is stored during a TS experiment (i.e. the value of ϵ/σ_0 after the creep and the recovery steps) is higher when T_σ is close to T_g .

Relevant information that may be analysed from Fig. 7 is the cooperative nature of the processes that were isolated using the TS procedure. It is well known that segmental motions involve cooperative conformational rearrangements [25]. However, when T_σ goes through the glassy state, one isolates mechanisms that are progressively simpler and that tend to an Arrhenius behaviour. In Adams and Gibbs theory [25], this would imply a freezing of the cooperative motions and thus the vanishing of the configurational entropy, S_c . In that case, the activation energy would tend to $N_A s_c^* \Delta\mu/S_c$, where N_A is the Avogadro's number, s_c^* is the entropy of the minimum number of particles able to rearrange cooperatively and $\Delta\mu$ is the activation energy per particle opposing a cooperative rearrangement of the liquid/glass structure. In this context, it would be interesting to conclude on the cooperative nature of the processes observed in the glassy state. Are such modes simple, involving only the motion of chains that do not interfere with the neighbouring groups of atoms or molecules? Or, on the contrary, do the molecular motions assigned to this process involve, in part, a range of related motions within an appreciable correlation volume? Starkweather formalism was shown to be a suitable tool for

assigning a relaxation as either “complex” (cooperative in nature) or “simple” (localised mobility) [26, 27]. This procedure is based on the use of the concept of activation entropy, ΔS , where the activation energy of the process is compared to the activation energy of a zero-entropy (non-cooperative) process. For the case of $\Delta S=0$, it can be shown that [26, 27]:

$$E_a = RT \left[1 + \ln \left(\frac{k_B T}{2\pi h f} \right) \right] \quad (5)$$

where f is the frequency of the experiment, k_B is the Boltzmann constant and h is the Planck constant. In TSR experiments, the equivalent frequency f can be assumed to be around $10^{-2.5}$ Hz [15]. The $E_a(T)$ line for the case of $\Delta S=0$ was added to the data in Fig. 7 (solid line). It can be seen that around T_g , the experimental values of E_a strongly deviate from the zero-entropy line. This would be expected because at such high temperatures the processes are highly cooperative. However, in the glassy region the values of E_a are lower but are still much higher than the ones given by the $\Delta S=0$ prediction. Moreover, from the trend of the results towards lower temperatures, it is not expected that the experimental values would reach a non-cooperative character. Such deviation from the non-cooperative behaviour in the glassy state has been observed in thermally stimulated results, including a similar polyester thermoset (with no styrene content) [28]. The values of E_a of the system studied in that work [28] are similar to the ones observed for UPR25 and UPR38. It should also be mentioned in this context that similar UPRs that were studied in the present work were analysed using TSDC, by Chebli et al. [29]. Also in that work, the values of E_a were of the same order of magnitude as the ones measured by TSR, and again strong deviation from the zero-entropy prediction was observed [29]; only at lower temperatures, the β relaxation exhibits a nearly non-cooperative character. We will use the $E_a(T)$ data obtained in this work to gather further information about the structural and dynamic features of the glass transition of such systems.

The classification of liquids as “strong” and “fragile” has been promoted by Angell to describe the relaxation in glass-forming systems [30]. One relevant parameter here is the fragility index, m , that is related to the rate at which the characteristic times, or other related property such as viscosity, decreases with increasing temperature at T_g , when plotted on a normalised T_g/T plot:

$$m = \left. \frac{d \log \tau}{d(T_g/T)} \right|_{T_g} = \frac{E_a(T_g)}{\ln(10)RT_g} \quad (6)$$

Values of $m=16$ correspond to Arrhenius behaviour (strong limit) and for $m>200$ the system reaches the fragile limit, where a strong curvature is found in the Angell plot ($\log \tau$ versus T_g/T) [31].

There are different ways of determining the fragility of glass-forming liquids. However, when one pretends to quantify it, the final results may depend upon the technique and calculation procedure used. It was suggested that the $E_a(T)$ data obtained from TSR could be a suitable method to infer the fragility of polymer systems [16]. However, when m is calculated from DSC, DMA and TSR data on the same system, we end up with different values, that reflect the different thermal history of the sample and the physical probe used to determine the dynamics of the system [16, 23]. Other reasons can explain these differences, including our definition of $\tau(T_g) = 100$ s, which is known to be not an universal value and depending on the method used can vary from 10^{-3} to 100 s [32]. As the value of m is related to the slope of $\ln(\tau)$ at T_g , some fluctuation of the T_g temperature can give important differences for the value of m . This problem is not sensitive for measurements performed on strong or very strong liquids but is very important for fragile materials.

In this work, we also used the data from Fig. 7 to calculate the fragility indexes of UPR25 and UPR38. The T_g was estimated at the maximum of $E_a(T)$, using in this case the DMA results (isothermal data), yielding 86.0 and 95.4 for UPR25 and UPR38, respectively. Such values are very close to the calorimetric T_g s (83 and 95 °C [13]). From the values of E_a at such maximum temperatures of the DMA results, (Table 1) it may be possible to calculate m , using Eq. 6 (Table 1). We should discuss here the time scale at which the transition from the liquid region (in equilibrium) to the glassy region (non-equilibrium) takes place, which occurs at the temperature of maximum $E_a(T)$. In the DMA data, this should be dependent upon the equilibration time between each isothermal frequency scan: if we keep the sample for a longer time between each experiment, we can study the system in equilibrium during longer times, i.e. down to lower temperatures. In this work, the sample rested about 10 min between each experiment, which is quite compatible with the time scale of a DSC experiment. This could be the reason why the maximum of $E_a(T)$ observed by DMA is similar to the calorimetric T_g .

One could also use the maximum values of E_a obtained from the TS experiments, or the values of E_a of the TS experiments that exhibit the highest creep plateau (i.e. the highest values of ϵ/σ_0 before the final recovery

process during heating). A similar procedure was used in TSDC experiments to estimate the fragility index [33]. As discussed previously, the values of E_a determined from TSR are lower than the ones obtained from DMA. Therefore, one would obtain lower values of m , as the difference in the temperatures of maximum E_a observed from the TS and DMA results is not significant for the calculations. In this context, it would be interesting to compare the obtained values of m with the ones obtained by DSC [13] and dielectric relaxation spectroscopy [34]. Table 1 shows the compiled results. It can be concluded that DSC gives the highest values for fragility and DMA the lowest. The variations of fragility values observed between these two samples are coherent with the structure engaged. Indeed, the greater the styrene content, the greater the average length of the lateral chain; thus, the greater the cooperative domains implied in the relaxation process, as a consequence, the greater the fragility [35].

Conclusions

This work demonstrated that mechanical spectroscopic methods are adequate for studying the glass transition dynamics in unsaturated polyester polymers, being sensitive to the styrene content that was cured with the resin. As found in previous calorimetric and dielectric studies, T_g was found to increase with increasing styrene content. TSR tests were successfully implemented in the study of segmental mobility in such thermosets. The relaxation plots obtained from TS experiments allowed to calculate the temperature dependence of the apparent activation energy. The values obtained for E_a were similar to those obtained by dielectric methods and from TSR experiments performed in an equivalent system (without styrene). The $E_a(T)$ trend observed was explained taking into account the temperature dependence of the retardation times. TSR experiments probe the conformational cooperative mobility at time scales of the order of 100 s. Then, the Arrhenius plot undergoes a progressive change from the VFTH behaviour (in the liquid state) towards an Arrhenius regime (in the glassy state) at experiments near T_g . At such time scales, the activation energies of the processes activated at different temperature windows present a peak, with a maximum around T_g . The same trend was observed in the dynamic results (DMA). Such data was used to examine the fragile nature of the systems. It was found that the fragility index, m , is higher for the polymer with more styrene (rigid segments), which was attributed to the increase of the cooperative domains associated with the segmental mobility due to the increase of the average styrenic chain length; the same behaviour has already been reported from DSC and dielectric relaxation experiments.

Table 1 Information obtained from the data in Fig. 7 (DMA results) and values of m obtained from different techniques

	UPR25	UPR38	Reference
$T_g/^\circ\text{C}$	86.0	95.4	This work (DMA)
$E_a(T_g)/\text{kJ.mol}^{-1}$	385	430	This work (DMA)
$m(\text{DMA})$	56	61	This work (DMA)
$m(\text{DSC})$	91	135	[13]
$m(\text{dielectric})$	64	92–113	[32]

Acknowledgements The authors thank J.-P. Cahon for the support in the mechanical spectroscopy experiments (in the context of a European Socrates Erasmus student mobility grant) and Fabrice

Gouanve (equipe membrane, UMR3522 Rouen) for the synthesis. Financial support for this work was provided by FCT, through the POCTI and FEDER programmes.

References

- Richert R, Blumen A (eds) (1994) Disordered effects on relaxational processes. Springer, Berlin Heidelberg New York
- Proceedings of the 1st International Conferences on Relaxation in Complex Systems, Heraklion, 1990. *J Non-Cryst Solids* Vol. 131–133 (1991)
- Proceedings of the 2nd International Conferences on Relaxation in Complex Systems, Alicante, 1993. *J Non-Cryst Solids* Vol. 170–172 (1997)
- Proceedings of the 3rd International Conferences on Relaxation in Complex Systems, Vigo, 1997. *J Non-Cryst Solids* Vol. 235–237 (1998)
- Proceedings of the 4th International Conferences on Relaxation in Complex Systems, Hersonissos, 2001. *J Non-Cryst Solids* Vol. 307–310 (2002)
- Moynihan CT, Macedo PB, Montrose CJ, Gupta PK, DeBolt MA, Dill JF, Dom BE, Drake PW, Esteal AJ, Elterman PB, Moeller RP, Sasabe H (1976) *Ann N Y Acad Sci* 279:15
- Ferry JD (1980) Viscoelastic properties of polymers. Wiley, New York
- Mano JF, Viana JC (2001) *Polym Test* 20:937
- van Turnhout J (1975) Thermally stimulated discharge of polymer electrets. Elsevier, Amsterdam
- Alves NM, Mano JF, Gómez Ribelles JL (2002) *J Therm Anal Calorim* 70:633
- Alves NM, Mano JF, Gómez Ribelles JL (2002) *Polymer* 43:3627
- Bureau E, Chebli K, Cabot C, Saiter JM, Dreux F, Marais S, Metayer M (2001) *Eur Polym J* 37:2169
- Delahaye N, Marais S, Saiter JM, Metayer M (1998) *J Appl Polym Sci* 67:695
- Mano JF, Cahon J-P (2004) *Polym Test* 23:423
- Mano JF (1999) *Thermochimica Acta* 332:161
- Alves NM, Mano JF, Gómez Ribelles JL, Gómez Tejedor JA (2004) *Polymer* 45:1007
- Vogel H (1921) *Phys Z* 22:645
- Tamman G, Hesse W (1926) *Anorg Allg Chem* 156:245
- Fulcher GS (1925) *J Am Ceram Soc* 77:3701
- Mano JF, Correia NT, Moura Ramos JJ (1995) *J Chem Soc Farad Trans* 91:2003
- Sauer BB, Kim YH (1997) *Macromolecules* 30:3323
- Doulut S, Demont P, Lacabanne C (2000) *Macromolecules* 33:3425
- Alves NM, Gómez Ribelles JL, Gómez Tejedor JA, Mano JF (2004) *Macromolecules* 37:3735
- Halpern V (1993) *J Phys D Appl Phys* 26:307
- Adams G, Gibbs JH (1965) *J Chem Phys* 43:139
- Starkweather HW (1981) *Macromolecules* 14:1277
- Starkweather HW (1988) *Macromolecules* 21:1798
- Alves NM, Mano JF, Gómez Ribelles JL (2001) *Mat Res Innovat* 4:170
- Chebi K, Marais S, Saiter JM, Pardo EF, Grenet J, Metayer M (2000) *J Therm Anal Calorim* 62:657
- Angell CA (1991) *J Non-Cryst Solid* 131–133:13
- Böhmer R, Ngai KL, Angell CA, Plazek DJ (1993) *J Chem Phys* 99:4201
- Saiter JM, Dargent E, Kattan M, Cabot C, Grenet J (2003) *Polymer* 44:3995
- Correia NT, Alvarez C, Moura Ramos JJ, Descamps M (2000) *Chem Phys* 252:151
- Saiter A, Bureau E, Zapolsky H, Marais S, Saiter JM (2002) *J Non-Cryst Solids* 307–310:738
- Saiter A, Bureau E, Zapolsky H, Marais S, Saiter JM (2004) *J Non-Cryst Solids* (in press)